Investigations of range accuracy for long-range three-dimensional active imaging

Xiuda Zhang (张秀达)*, Huimin Yan (严惠民), and Qin Zhou (周 琴)

State Key Laboratory of Modern Optical Instrument, National Engineering Research Center for Optical Instrument, Optical Engineering Department, Zhejiang University, Hangzhou 310027, China

**Corresponding author: zjuzxd@yahoo.com.cn*

Received November 30, 2010; accepted January 14, 2011; posted online April 28, 2011

Distance resolutions and noises are analyzed experimentally for long-range three-dimensional (3D) active imaging systems that have signal-to-noise ratios (SNRs) more optimal than 30:1. Findings indicate that the photon shot noise primarily determines the SNR. However, the active imaging method, which has a relatively low SNR, generates a relatively high distance resolution. To explain this phenomenon, a theory in which the distance resolution of 3D active imaging systems is determined by both the photon shot noise and the subinterval width is developed. Theoretical and experimental results differ by less than 4%.

OCIS codes: 110.6880, 120.0280.
doi: 10.3788/COL201109.061101.

"Range-gated" or three-dimensional (3D) active imaging, in several cases, has been discussed and demonstrated in experimental studies for more than a decade. In recent years, various methods, such as the gain-modulated method[1−4], time slicing method[5,6], and super-resolution method[7], have been proposed to increase the speed of measurement, improve the distance resolution or to attain a combination of both for 3D active imaging. However, distance resolutions by these methods rely on the signal-to-noise ratio (SNR) of the active imaging intensity images[8]. To obtain relatively high "electric-to-light" transfer efficiency of laser diodes (LDs), these 3D active imaging systems, which employ LDs as the light source[2,7], have been designed with relatively high illumination light output power; thus, they have a relatively high SNR than systems that employ a Q-switched laser as the light source. In addition, with regard to the low coherence property, LD-based 3D active imaging systems are "almost" unaffected by laser speckle[8], which influences Q-switched laser-based systems. For relatively low SNR, 3D active imaging systems have been analyzed[3,6,8], and high SNR data have been found to be more valuable for applications. The following analysis exclusively considers LD-based 3D imaging systems.

The super-resolution depth-mapping 3D imaging method has a distance resolution ten times superior to that of the conventional active imaging method in the same detection times[7]. Laurenzis *et al.* achieved these results by employing a rectangularly-shaped laser pulse and gate gain[1]. Further, the pulse-shape-free linearity method[2] achieved super-resolution depth mapping by using a linearly modulated gain receiver and arbitrary shape of pulses. In several practical systems, the receiver noise can be approximated by a Gaussian distribution. If the receiver noise obeys the Gaussian distribution and has a standard diversion of σ, two objects can be distinguished by their differences when the distance between them is greater than 3σ[1]. In long-range 3D detections, two imaging systems[2,7] have been reported to obtain intensity images that have a SNR more optimal than 30:1 for both bright and dark objects; this is because they achieved super-resolution depth mapping. The photon's SNR is directly related to the square of the photon number; this is because the photons received by the 3D system obey Poisson distribution. The photon number that the 3D systems receive should be at least 900. Further, the photon number should be more than 900 for the practical detector quantum efficiency is less than 100%.

Figure 1 shows the intensity-to-time profiles of the super-resolution detection method and the pulse-shape-free linearity method. From Fig. 1(a), it is apparent that the super-resolution detection method[6] has three areas in the intensity-to-time profiles of each time of detection: the rising ramp area, the plateau area, and the falling ramp area. To distinguish these three areas, the relative value of the same pixel can be used in two different intensity images obtained by different gated delays. Further, from Fig. 1(a), if $I_{\rm a1} > I_{\rm a2} > 0$ ($I_{\rm a1}$ and $I_{\rm a2}$ are the intensities of images a1 and a2, respectively), then the plateau area is the point for the first detection and the rising ramp area for the second detection; however, if $0 < I_{\rm a1} < I_{\rm a2}$, then the falling ramp area is the point of the first detection and the plateau area for the second detection. The depth is the quotient of the trapezoid value divided by the ramp value, and the ramp includes both rising and falling ramps. The super-resolution detection method[7] uses two equations to calculate the depth of objects. The pulse-shape-free linearity method[2] uses one equation because it only has a rising ramp, as depicted in Fig. 1(b). From these discussions, the gate subinterval can be defined as an area in which the distance is a monotonic function with the ratio of two intensities. That is, in the gate subinterval, the distance is a monotone that increases or decreases with the quotient of the two intensities. In the super-resolution method, the subinterval width is the step-time width; however, in the pulse-shape-free linearity method, the subinterval width is the gate-time width.

In order to test their distance-detection performances,

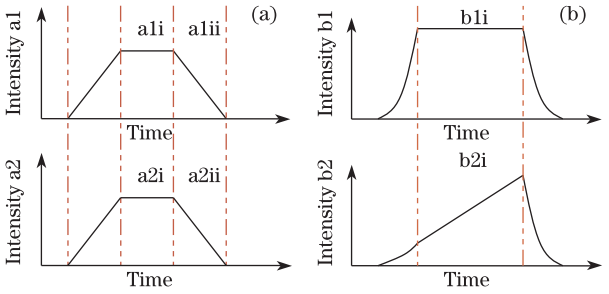

Fig. 1. Intensity to time profiles of (a) the super-resolution method and (b) the pulse-shape-free linearity method.

Table 1. Experimental Results of 3D Imaging Systems

	Super-Resolution 3D Imaging System	Pulse-Shape-Free Linearity 3D Imaging System
SNR of Intensity Image 1	45.1:1	44.8:1
SNR of Intensity Image 2	27.5:1	43.3:1
Distance Resolution (m)	3.27	5.02

Table 2. Theoretical Results Obtained for 3D Imaging Systems

	Super-Resolution 3D Imaging System	Pulse-Shape-Free Linearity 3D Imaging System
SNR of Intensity Image 1	49.3:1	49.3:1
SNR of Intensity Image 2	32.3:1	49.3:1
Distance Resolution (m)	3.19	4.82

a super-resolution 3D imaging system and a pulse-shape-free linearity 3D imaging system were constructed. Both systems were designed to have the same parameters, and they both employed quasi-continuous-wave (QCW) LD stacks as the pulsed light source with peak powers of 2.4 kW at 808 nm and average laser powers of approximately 21.0 W. The charge-coupled device (CCD) cameras had a resolution of 1,000×1,000 (pixels) at a frame rate of 7.5 frames per second (fps) and the gate times were equivalent to 1 μs for both systems. The detection object selected was a plane wall situated at a distance of 1 km. The optics diameter of the receiver was 120 mm and the receiver transmission was approximately 91%. The backscattering could be neglected for the gate[9−12]. Under good weather conditions, the influence of the atmospheric turbulence can be neglected[13−17]. Both systems detected a wall on a clear night. The results obtained by this detection are presented in Table 1. Further, the parameters were used to calculate the average photon number per pixel; thus, the shot noises and the corresponding distance resolutions were obtained. The results obtained from calculations are documented in Table 2.

From Tables 1 and 2, it can be concluded that the SNR of photon shot noise primarily determines the SNR of the intensity noise on such an occasion. Gate jitter[6] and modulation instability of the micro-channel plate[17,18] can be neglected when the gate width measures tens of nanoseconds to several microseconds. It has been discussed previously that, if the signal photon number is greater than 900, the equivalent background input (EBI) noise of the image intensifier and the noise of the CCD camera[19] can be neglected. Although the shot noise obeys the Poisson distribution, it trends to the Gaussian distribution when the photon number is sufficiently large. This verifies the assumption that the noise obeys the Gaussian distribution.

The super-resolution imaging system has the same SNR for the first image as compared with the pulse-shape-free linearity system; however, the super-resolution imaging system has a lower SNR in the second image. For the super-resolution imaging system, the gate permits only a part of the pulse energy to enter and, thus, reduces the photon number and decreases the SNR of photons in the second detection. Therefore, the second image has a lower SNR. However, the super-resolution method has a better distance resolution. Although the SNR of the intensity image determines the fraction number into which the gate range can be divided, the detection range has been divided into two sub-ranges for the super-resolution imaging system; however, there is no sub-range for the pulse-shape-free linearity 3D imaging system. This is because the subinterval is an area where the distance is a monotonic function with the ratio of two intensities, and the super-resolution method gets two depth subintervals whereas the pulse-shape-free method gets one subinterval. Thus, the super-resolution 3D imaging system obtains a higher distance resolution than the pulse-shape-free linearity method under the same conditions. In the super-resolution method, the ramp is the correlation of the gate and the pulse. Therefore, the gate subinterval width is determined by the shorter one of the pulse width and the gate width. Based on the above discussion, the expression of the distance resolution in theory can be obtained as follows.

The photon shot noise mainly influences the SNR of intensity images. Both methods obtain the distance as

$$z \propto I_1/I_2, \tag{1}$$

where I_1 and I_2 are the gray levels of the first and the second intensity images, respectively.

From previous discussions, the SNR of the intensity image is mainly determined by photon shot noise and the SNR is much larger than 1. Taking into account these two points and Eq. (1), the distance can be seen to obey

$$\delta \propto \sqrt{1/N_1 + 1/N_2}, \tag{2}$$

where N_1 and N_2 are the average photon numbers per pixel of the first and the second intensity images, respectively. From Refs. [2] and [7], it is obvious that the distance resolution also has a direct ratio to the gate subinterval width. Therefore, the "average" depth resolution is

$$\delta = \frac{\Lambda}{2}\sqrt{1/N_1 + 1/N_2}, \tag{3}$$

where Λ=$cT/2$ is the gate subinterval distance width, c is the speed of light, and T is the gate subinterval time width.

If the object distance is close to the junctional area of the gate, it should be noted that other noises will prominently influence the distance resolution. Table 2, in addition, shows the theoretical distance resolution, which is calculated by Eq. (3). When comparing the theoretical and experimental results, a 2.45% error is observed for the super-resolution 3D imaging system and a 3.98% error for the pulse-shape-free linearity 3D imaging system. These results validate Eq. (3), which demonstrates that both the photon shot noise and the subinterval width determine the distance resolution of the long-range 3D active imaging systems.

From Eq. (3), it can be observed that increasing the photon number is one method to improve the distance resolution. The large-value photon number indicates a large output power from the light source. Further, from Eq. (3), one enlarges 100 times of the photon number to obtain only 10 times better distance resolution. Another method to improve the distance resolution is to shorten the subinterval width. However, the shorter subinterval width indicates a smaller detection depth range. A longer detection time can be employed to enlarge the detection depth range; however, the detection speed will decrease as a consequence. Therefore, the method obtains a larger subinterval number in the same detection time and can obtain a higher distance resolution in the same detection depth range or obtain a larger detection-depth range in the same distance resolution.

In conclusion, the input shot noise of the image intensifier is identified to be the main factor which influences the SNR of the high-SNR 3D imaging systems. The distance resolution of the 3D active imaging systems is determined by the photon shot noise and the subinterval width.

This work was supported by the National "863" Program of China (No. 2009AA12Z142) and the National Natural Science Foundation of China (No. 40901166).

References

1. M. Kawakita, K. Iizuka, R. Iwama, K. Takizawa, H. Kikuchi, and F. Sato, Opt. Express **12,** 5336 (2004).
2. X. Zhang, H. Yan, and Y. Jiang, Opt. Lett. **33,** 1219 (2008).
3. C. Jin, X. Sun, Y. Zhao, Y. Zhang, and L. Liu, Opt. Lett. **34,** 3550 (2009).
4. J. Yao, H. Yan, X. Zhang, and Y. Jiang, Chinese J. Lasers (in Chinese) **37,** 1613 (2010).
5. J. F. Andersen, J. Busck, and H. Heiselberg, Appl. Opt. **45,** 6198 (2006).
6. P. Andersson, Opt. Eng. **45,** 034301 (2006).
7. M. Laurenzis, F. Christnacher, and D. Monnin, Opt. Lett. **32,** 3146 (2007).
8. E. Repasi, P. Lutzmann, O. Steinvall, M. Elmqvist, B. Gohler, and G. Anstett, Appl. Opt. **48,** 5956 (2009).
9. O. Steinvall, H. Olsson, G. Bolander, C. Carlsson, and D. Letalick, Proc. SPIE **3707,** 432 (1999).
10. R. Vollmerhausen, E. Jacobs, N. Devitt, T. Maurer, and C. Halford, Proc. SPIE **5076,** 101 (2003).
11. R. L. Espinola, E. L. Jacobs, C. E. Halford, R. Vollmerhausen, and D. H. Tofsted, Opt. Express **15,** 3816 (2007).
12. E. L. Jacobs, R. H. Vollmerhausen, and C. E. Halford, Proc. SPIE **5407,** 201 (2004).
13. E. Golbraikh and N. S. Kopeika, Appl. Opt. **43,** 6151 (2004).
14. Z. Zalevsky, S. Rozental, and M. Meller, Opt. Lett. **32,** 1072 (2007).
15. Z. Tao, Q. Zhang, K. Yuan, D. Wu, K. Cao, S. Hu, and H. Hu, Chin. Opt. Lett. **8,** 732 (2010).
16. W. Gong, J. Zhang, F. Mao, and J. Li, Chin. Opt. Lett. **8,** 533 (2010).
17. I. P. Csorba, Appl. Opt. **19,** 3863 (1980).
18. G. Murakami, K. Yoshioka, and I. Yoshikawa, Appl. Opt. **49,** 2985 (2010).
19. D. L. Snyder, C. W. Helstrom, A. D. Lanterman, M. Faisal, and R. L. White, J. Opt. Soc. Am. A **12,** 272 (1995).